NiS_2-Integrated Cd-Oxalate MOF: A Multifunctional Platform for Selective 2,4-D Amine Sensing and Efficient NR/EBT Photodegradation

Azaz Ahmed[a], Musheer Ahmad[b], Chandrakant Thakur[c], Astakala Anil Kumar[d], Nohyun Lee[d], Nazrul Haq[e], Kafeel Ahmad Siddiqui[a]

[a] Department of Chemistry, National Institute of Technology Raipur, G. E. Road Raipur – 492010, Chhattisgarh, India.

[b] Department of Applied Chemistry, Faculty of Engineering and Technology, ZHCET, Aligarh Muslim University, Aligarh, UP (India) – 202002.

[c] Department of Chemical Engineering, National Institute of Technology Raipur, G. E. Road Raipur - 492010, Chhattisgarh, India.

[d] School of Advanced Materials Engineering, Kookmin University, Seoul 02707, South Korea.

[e] Department of Pharmaceutics, College of Pharmacy, King Saud University, Riyadh 11451, Saudi Arabia.

[a] Corresponding Author: Dr. Kafeel Ahmad Siddiqui

[a] e-mail: kasiddiqui.chy@nitrr.ac.in

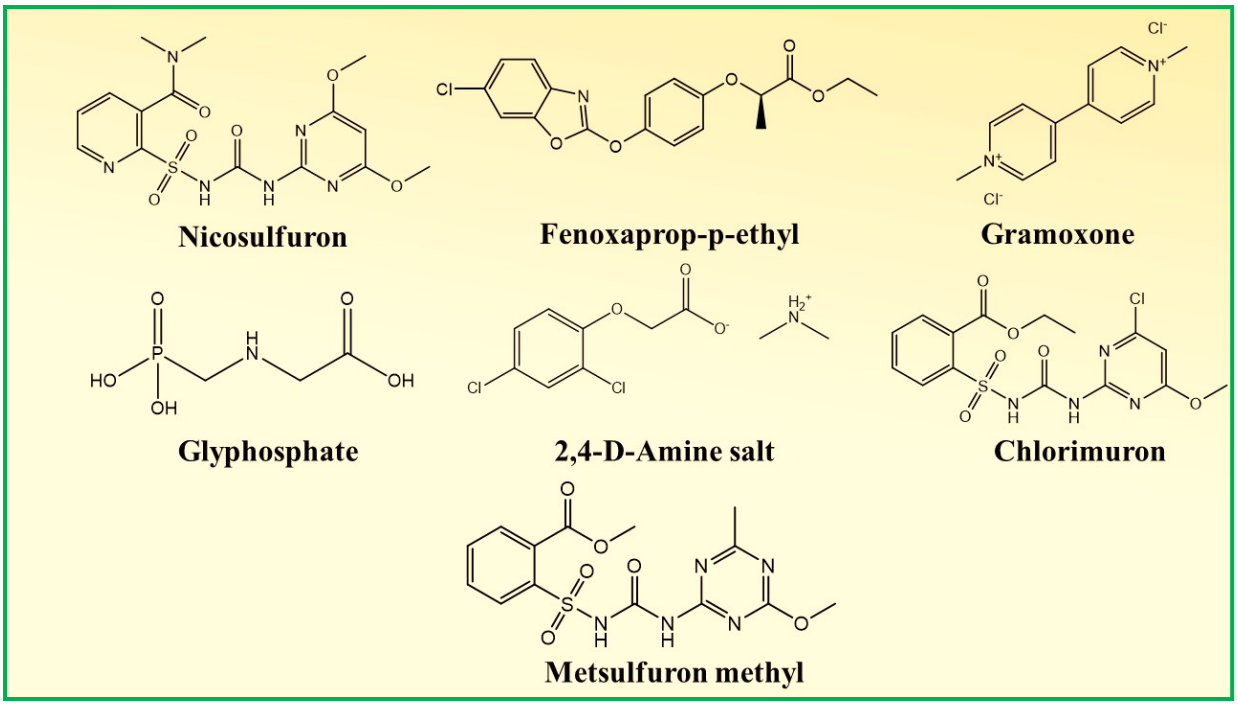

Fig.S1. Chemical structure of Herbicides.

Table S1. The names and corresponding chemical structures of the dyes employed in this study are provided.

S.No.	Dye	Dye Structure	λ_{max} (nm)
Cationic			
1.	Methyl Violet	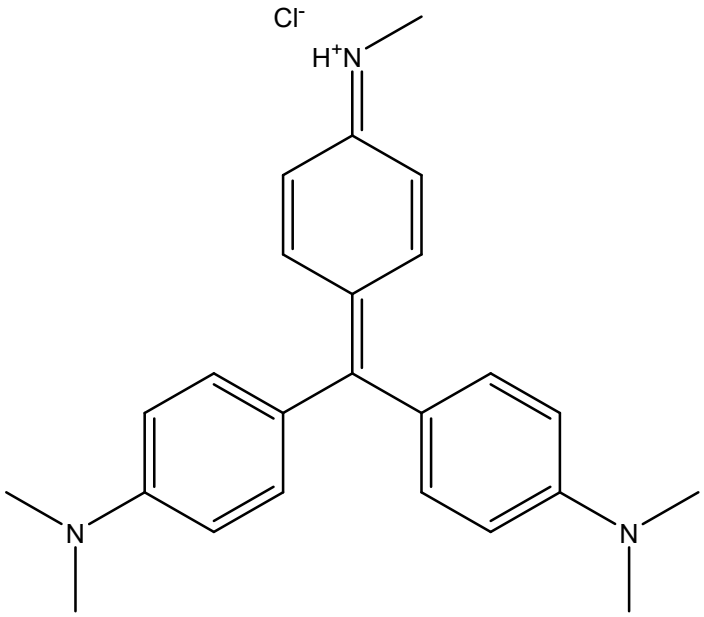	**589.49**
2.	Crystal Violet	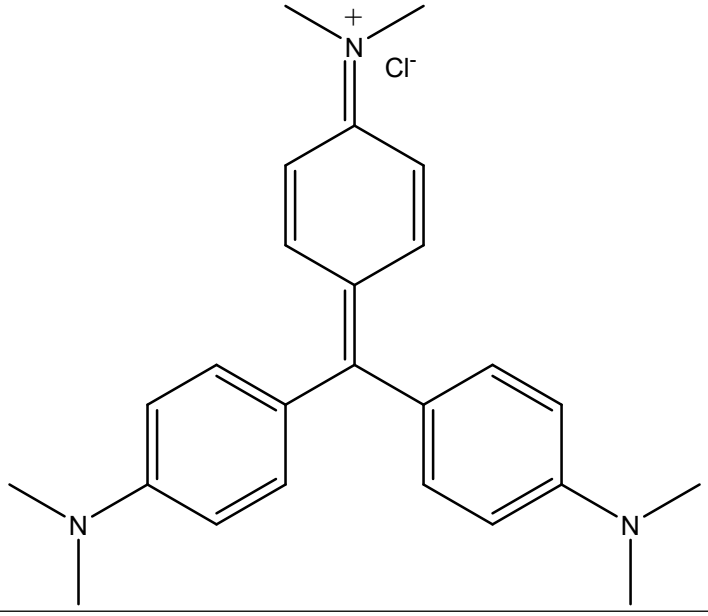	**590.67**

3.	Rhodamine B	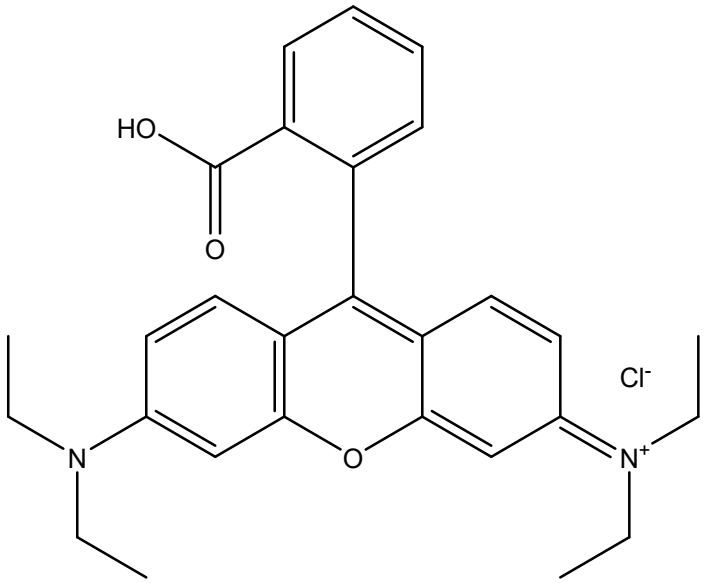	**553.24**
4.	Rhodamine 6G	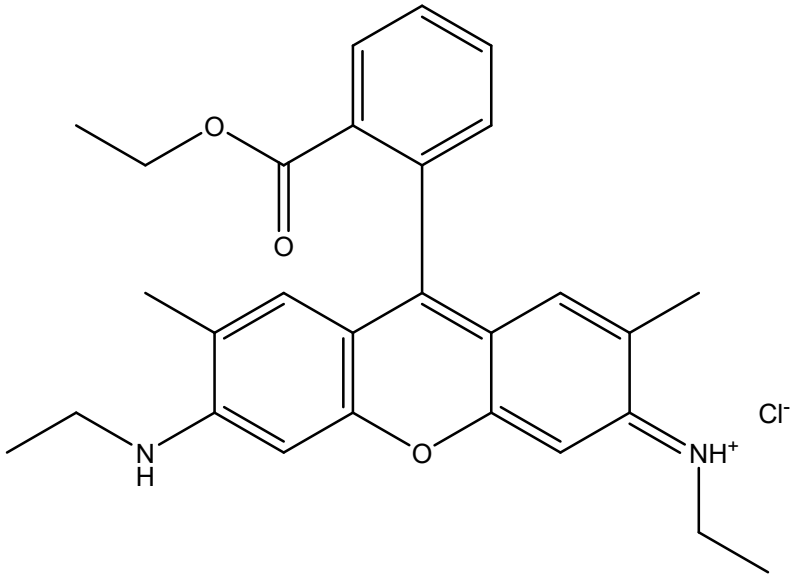	**525.31**
5.	Safranin O	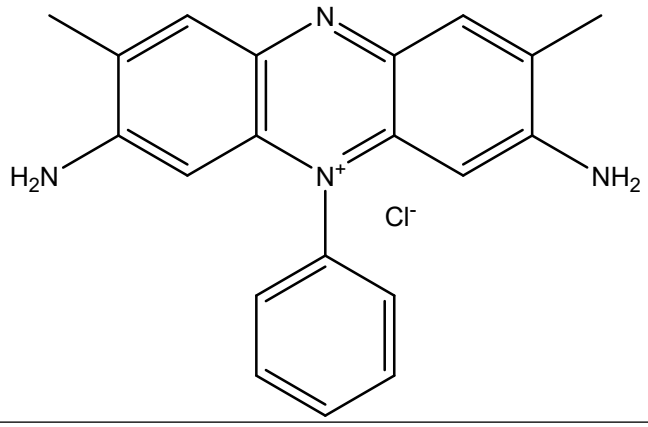	**519.58**

6.	Methyl Blue	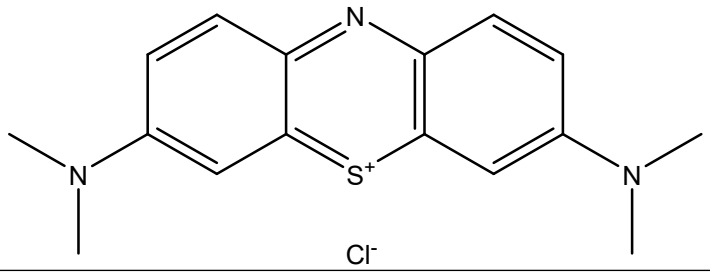	**662.63**
		Anionic	
7.	Rose Bengal	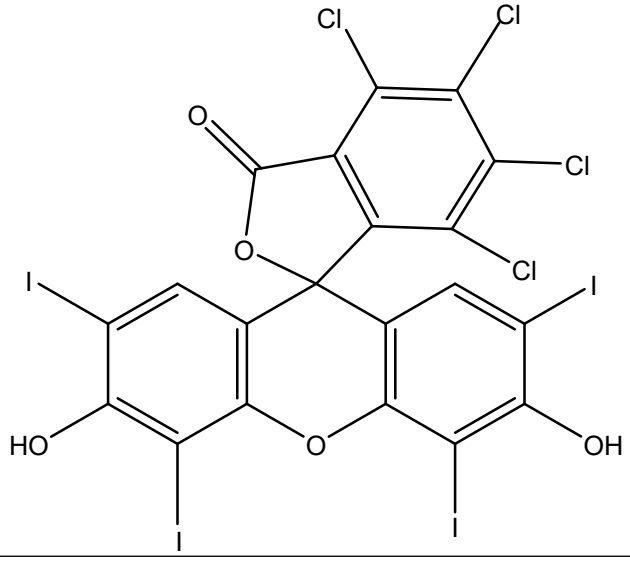	**549.44**
8.	Eriochrome Black T	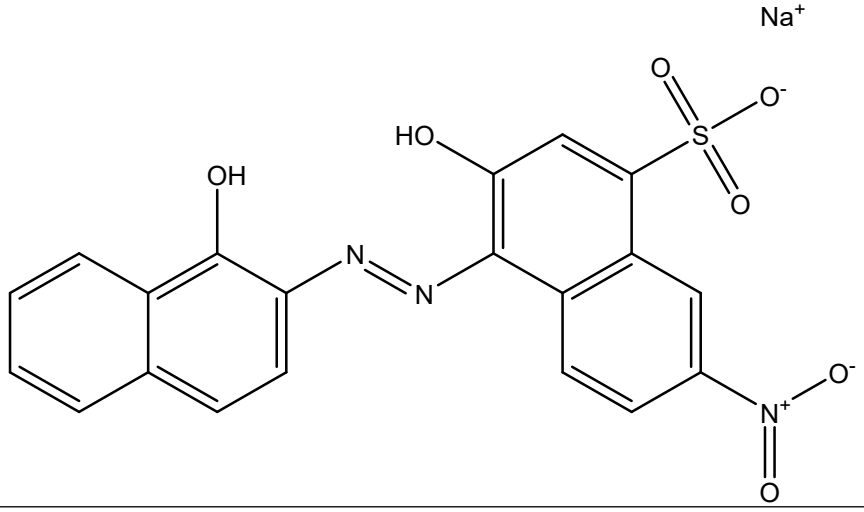	**529.23**

9.	Congo Red	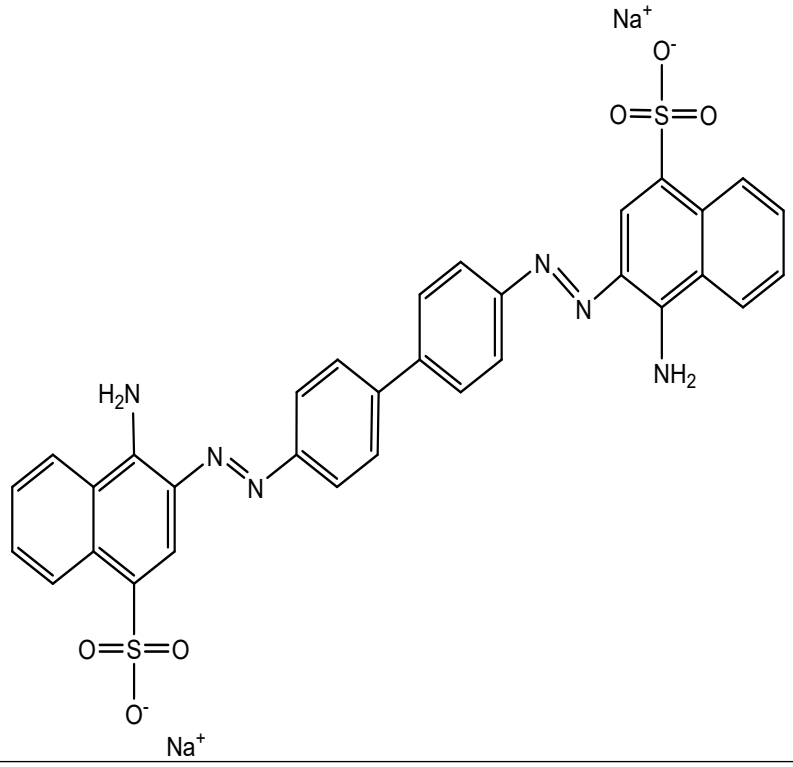	**497.82**
10.	Methyl Orange	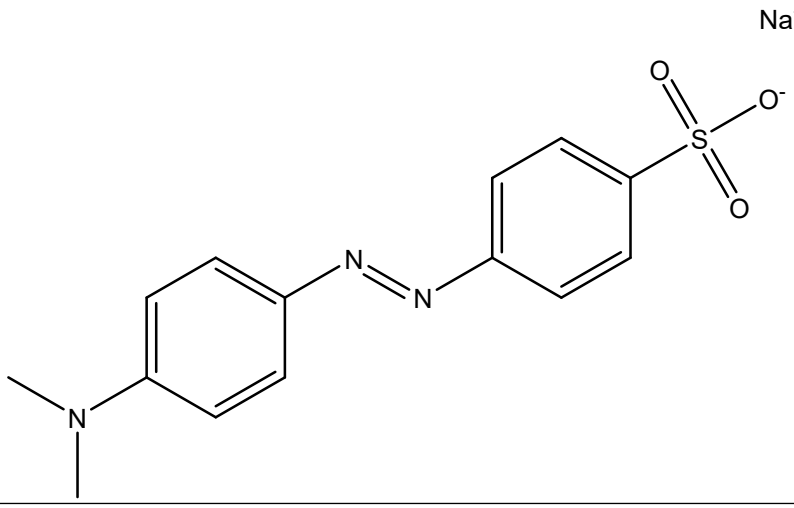	**463.43**

11.	Bromophenol Blue	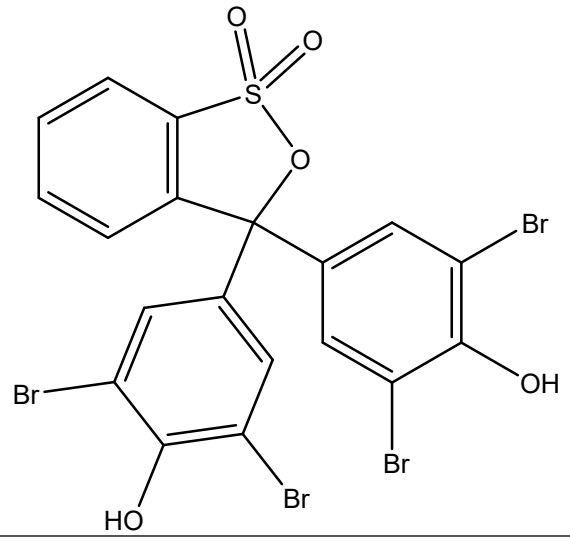	**591.75**
		Neutral	
12.	Neutral Red	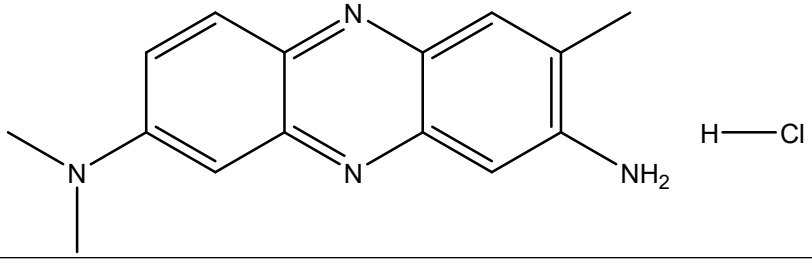	**532.86**
13.	Fluorescein	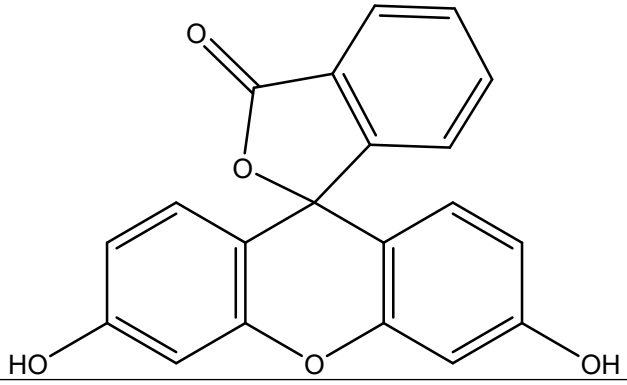	**483.51**

Table S2. Crystal data and structure refinement for **Cd-MOF**

Identification code	**Cd-MOF**
Empirical formula	$C_2H_6CdO_7$
Formula weight	254.48
Temperature/K	293(2)
Crystal system	triclinic
Space group	P-1
a/Å	6.00275(8)
b/Å	6.65883(6)
c/Å	8.48721(10)

α/°	74.6832(9)
β/°	74.3039(11)
γ/°	81.0102(9)
Volume/Å^3	313.678(6)
Z	2
ρ_{calc}g/cm^3	2.6941
μ/mm^{-1}	3.465
F(000)	242.6
Crystal size/mm^3	0.47 × 0.29 × 0.17
Radiation	Mo Kα (λ = 0.71073)
2Θ range for data collection/°	5.12 to 54.84
Index ranges	-7 ≤ h ≤ 7, -8 ≤ k ≤ 8, -10 ≤ l ≤ 10
Reflections collected	18351
Independent reflections	1380 [R_{int} = 0.1007, R_{sigma} = 0.0373]
Data/restraints/parameters	1380/0/97
Goodness-of-fit on F^2	1.071
Final R indexes [I>=2σ (I)]	R_1 = 0.0268, wR_2 = 0.0707
Final R indexes [all data]	R_1 = 0.0280, wR_2 = 0.0745
Largest diff. peak/hole / e Å^{-3}	0.99/-0.86
CCDC number	2484446

Table S3. Bond Lengths for **Cd-MOF**

Atom	Atom	Length/Å	Atom	Atom	Length/Å
Cd1	O2^1	2.354(2)	O2	C1	1.243(5)
Cd1	O4^2	2.368(3)	O4	C2	1.245(5)
Cd1	O3	2.377(2)	O3	C2	1.255(4)
Cd1	O3^3	2.360(3)	O1	C1	1.257(4)
Cd1	O1	2.296(3)	C1	C1^1	1.562(7)
Cd1	O6	2.350(3)	C2	C2^4	1.544(7)
Cd1	O5	2.288(4)			

Table S4. Bond Angles for **Cd-MOF**

Atom	Atom	Atom	Angle/°	Atom	Atom	Atom	Angle/°
O4^1	Cd1	O2^2	73.66(9)	O5	Cd1	O3^3	100.17(12)
O3	Cd1	O2^2	146.41(9)	O5	Cd1	O3	93.61(11)
O3^3	Cd1	O2^2	126.21(10)	O5	Cd1	O1	175.18(10)
O3^3	Cd1	O4^1	69.02(9)	O5	Cd1	O6	84.90(12)
O3	Cd1	O4^1	136.76(9)	C1	O2	Cd1^2	116.4(2)
O1	Cd1	O2^2	71.25(9)	C2	O4	Cd1^4	117.7(2)

O1	Cd1	O4[1]	105.74(11)	C2	O3	Cd1[3]	117.5(2)
O1	Cd1	O3[3]	83.12(10)	C2	O3	Cd1	132.9(2)
O1	Cd1	O3	84.13(10)	C1	O1	Cd1	117.8(3)
O6	Cd1	O2[2]	76.78(10)	O1	C1	O2	125.4(3)
O6	Cd1	O4[1]	139.08(10)	C1[2]	C1	O2	117.2(4)
O6	Cd1	O3[3]	151.51(9)	C1[2]	C1	O1	117.4(4)
O6	Cd1	O3	81.08(9)	O3	C2	O4	126.0(3)
O6	Cd1	O1	90.54(11)	C2[5]	C2	O4	117.0(4)
O5	Cd1	O2[2]	109.07(11)	C2[5]	C2	O3	117.0(4)
O5	Cd1	O4[1]	78.82(12)				

Table S5. Comparison of **Cd-MOF** and **NiS_2/Cd-MOF** with reported probes for 2,4-D amine salt (DAS)

S. No.	MOF-based Sensors	Objective	LOD	Reference
1	$[H_2BTC]^{2-}$. $[Zn(H_2O)_6]^{2+}$	DAS	0.351 ppm	9
2	Cd-MOF	DAS	0.665 ppm	This work
3	NiS_2/Cd-MOF	DAS	0.510 ppm	This work

detection in terms of sensitivity, selectivity, and detection limits.

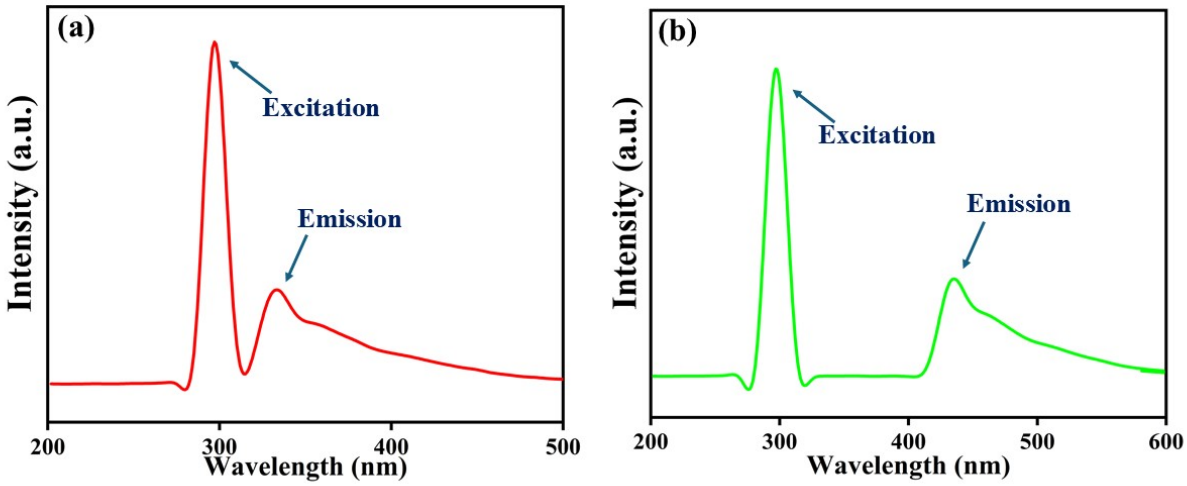

Fig.S2. Excitation and emission spectra of Cd-MOF and NiS_2/Cd-MOF in aqueous suspension, illustrating the strong fluorescence emission of (a) Cd-MOF at 332.65 nm and the red-shifted emission of (b) NiS_2/Cd-MOF at 433.26 nm upon excitation at 300 nm.

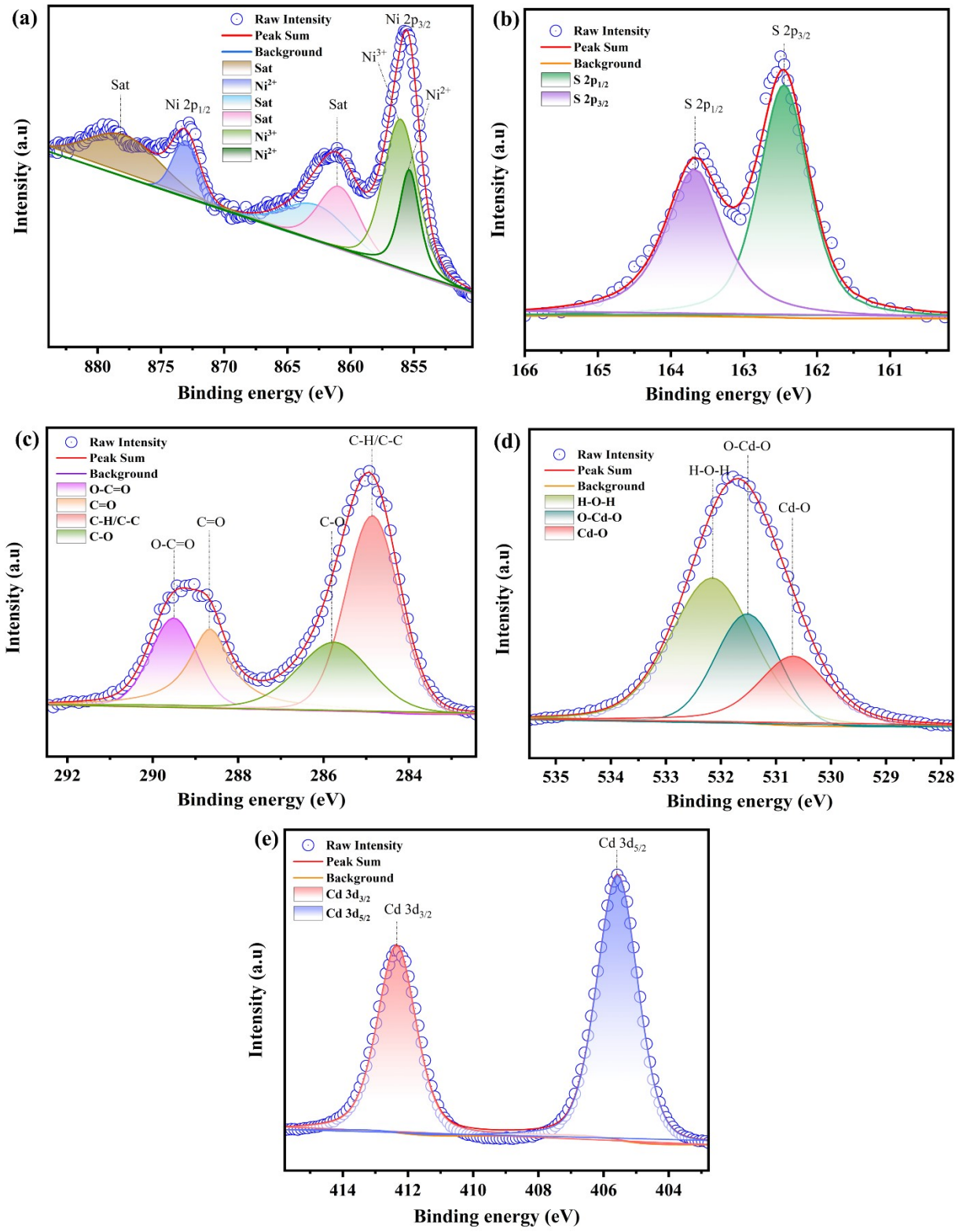

Fig. S3. High-resolution XPS spectra of pristine materials: (a) Ni 2p spectrum of NiS_2, (b) S 2p spectrum of NiS_2, (c) C 1s spectrum of Cd-MOF, (d) O 1s spectrum of Cd-MOF, and (e) Cd 3d

spectrum of Cd-MOF, confirming the chemical states and coordination environments of the constituent elements.

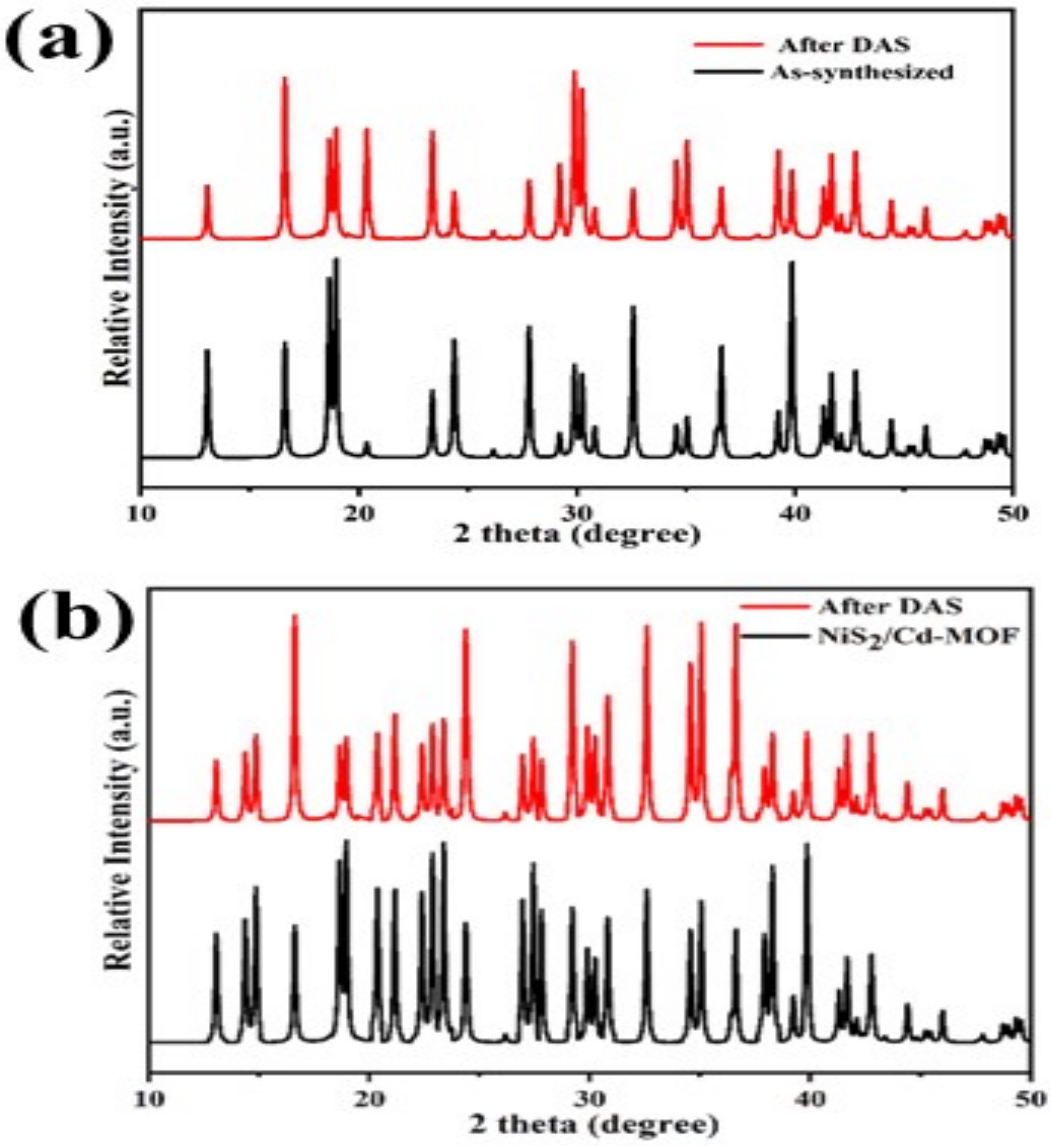

Fig.S4. PXRD patterns of the as-synthesized **Cd-MOF** and **NiS_2/Cd-MOF**, along with those recorded after sensing of (a) DAS and (b) DAS.

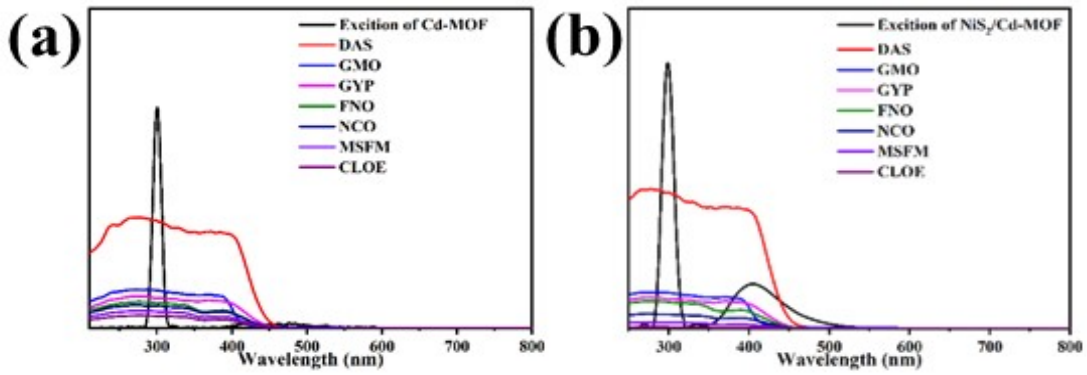

Fig.S5. Proposed fluorescence(FL) sensing mechanism of DAS using (a) **Cd-MOF** and (b) **NiS_2/Cd-MOF**

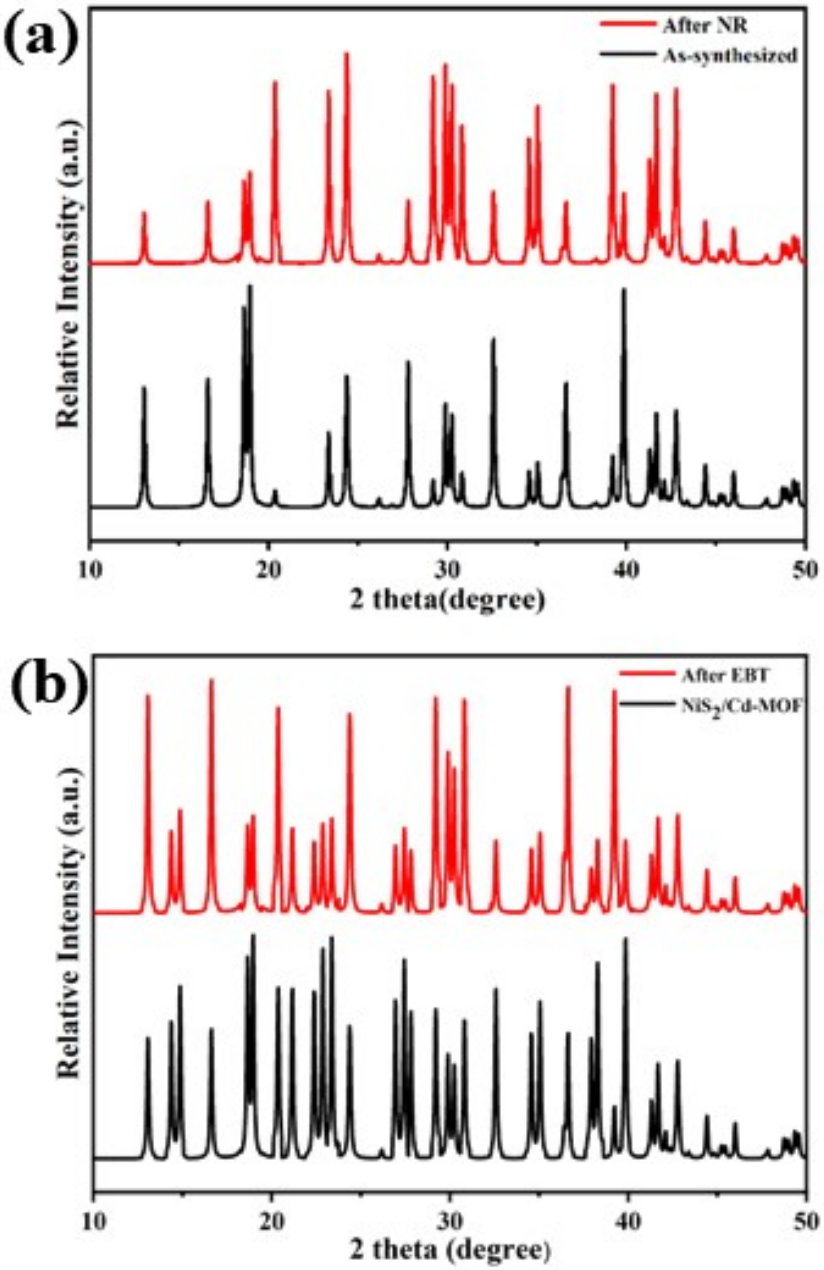

Fig.S6. PXRD patterns of (a) **Cd-MOF** after the degradation of NR and (b) **NiS_2/Cd-MOF** after the degradation of EBT.

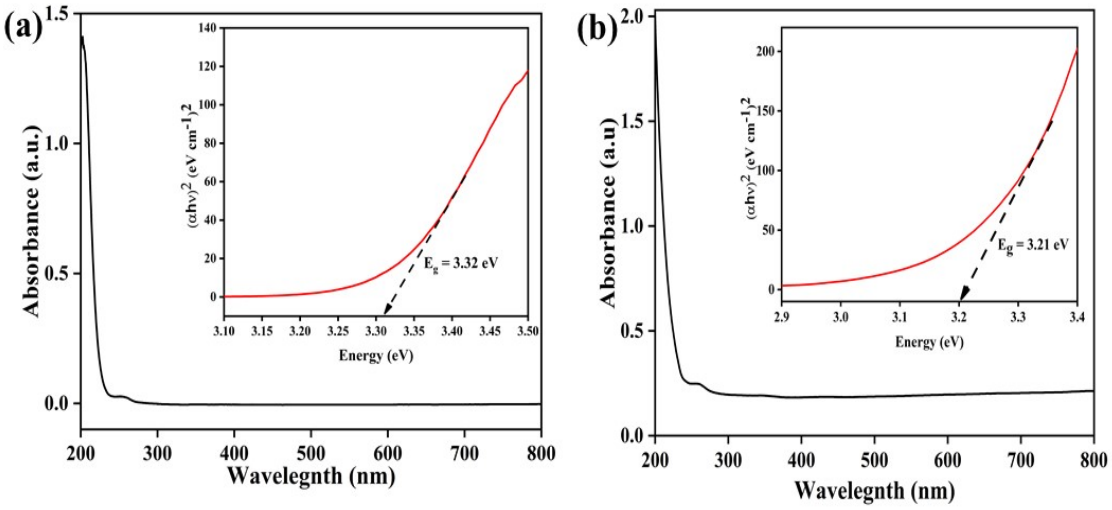

Fig.S7. UV-vis absorption spectra of (a) **Cd-MOF** and (b) **NiS_2/Cd-MOF**, with the corresponding Tauc plots shown in the insets.